Iron self-diffusion in amorphous FeZr/^{57}FeZr multilayers measured by neutron reflectometry

Mukul Gupta,[1,*] Ajay Gupta,[2] J. Stahn,[1] M. Horisberger,[1] T. Gutberlet,[1] and P. Allenspach[1]
[1]*Laboratory for Neutron Scattering, ETHZ and PSI, Paul Scherrer Institute, Villigen CH-5232, Switzerland*
[2]*Inter-University Consortium for DAE Facilities, Khandwa Road, Indore IN-452017, India*
(Received 19 May 2004; revised manuscript received 7 September 2004; published 18 November 2004)

Self-diffusion of iron in $^{natural}Fe_{67}Zr_{33}/^{57}Fe_{67}Zr_{33}$ multilayers has been investigated by neutron reflectometry. The as-deposited multilayer is amorphous in nature. It remains amorphous up to a temperature of 573 K and thereafter nanocrystallizes with an average grain size of 6 nm. The self-diffusion in the multilayers has been measured after isothermal vacuum annealing below the nanocrystallization temperature by monitoring the decay of the intensity of the first order Bragg peak, arising due to the isotopic periodicity. It has been found that the diffusivity at different temperatures follows an Arrhenius-type behavior with the preexponential factor $D_0 = 5 \times 10^{-18\pm1}$ m^2 s^{-1} and the activation energy $E = 0.38 \pm 0.05$ eV, respectively. These values of E and D_0 follow the well-known $E-D_0$ correlation and on the basis of this correlation it is suggested that diffusion mechanism in the present case is not highly collective but involves a rather small group of atoms.

DOI: 10.1103/PhysRevB.70.184206 PACS number(s): 66.30.Fq

I. INTRODUCTION

Amorphous metallic alloys also known as metallic glasses, are important from the point of their applications in industry for computers, information technology, recording media, etc.[1] They differ from their crystalline counterparts by a nearly random arrangement of atoms and are an example of the paradigm of dense random packing which leads to a great fundamental interest in these alloys.[2] Generally, these alloys are metastable, and at elevated temperatures various atomic rearrangements take place above their crystallization temperature T_x, the atomic mobility increases drastically causing a rapid crystallization, and even below T_x the amorphous matrix is internally unstable and transforms continuously to amorphous states of lower free energy. Transformation of a structure towards lower free energy is well-known as structural relaxation of amorphous structure and leads to changes in most of the physical properties. Atomic transport properties, such as diffusion are among the most affected during structural relaxation process and may change by several orders of magnitude.[3] This leads to a strong need for an understanding of the diffusion behavior in amorphous alloys. Because of their limited thermal stability it was not possible to study long range atomic transport in these alloys.

Various attempts have been made to increase the thermal stability of these alloys using a multicomponent matrix in bulk metallic glasses and melt spun ribbons. Self-diffusion measurements have been performed in a series of alloys, e.g., ZrCuNiTiBe,[4] CoFeNbB,[5] ZrCuNiAl[6] (and Ref. 2 and references therein). Some studies have also been done in binary amorphous alloys, e.g., NiZr,[7] CoZr,[8] TiZr,[9] etc. at temperatures >470 K. Most of these studies have been done using profiling and sectioning techniques such as radiotracer techniques, secondary ion mass spectroscopy (SIMS), Rutherford backscattering (RBS), Auger electron spectroscopy (AES), etc. Since the depth resolution available with these techniques is of the order of a few nm, diffusion length less than that could not be probed. Generally, the crystallization temperature in amorphous alloys is around 700 K which gives an upper limit for the diffusion annealing. Typical diffusion lengths at low temperatures (<400 K) in a reasonable time would be much shorter than the detection limit of cross-sectioning or depth-profiling techniques. In addition, for studying diffusion in amorphous ultrathin films (thickness $\sim$ few nm) a technique with greater sensitivity is required as the crystallization temperature in such layers is significantly lower as compared to bulk metallic glasses or melt-spun ribbons.

Measurement of interdiffusion in compositionally modulated multilayer structures using x-ray scattering is one technique to study diffusion lengths much shorter than the detection limit of sectioning and profiling techniques.[10–13] Several attempts have been made to study interdiffusion in chemically inhomogeneous multilayers. In a study by Mizoguchi *et al.*,[14] interdiffusion and structural relaxation have been studied in 3*d* transition metal (TM)/Zr multilayers in the composition range of $TM_{67}Zr_{33}$ using x-ray diffraction (XRD) technique. Amorphization in these multilayers has been achieved with a solid state reaction and diffusion measurements were performed at temperatures as low as 393 K. In another study Wang *et al.*[15] have studied interdiffusion in nanometer-scale multilayers using low-angle x-ray diffraction in a series of polycrystalline binary alloys. While x-ray diffraction/reflection techniques can be successfully used for interdiffusion studies in chemical-composition modulated multilayers, they cannot be used for studying self-diffusion in a chemically homogeneous structure because of electronic interaction with x-rays.

Neutron reflectivity is a nondestructive technique, which can be used for studying self-diffusion in a chemically homogeneous multilayer with a resolution as small as 0.1 nm, by taking advantage of isotopic labeling. Greer *et al.*[10,16,17] have demonstrated the application of neutron reflectivity, measuring self-diffusion in amorphous NiZr multilayers. In another study by Baker *et al.*[18] self-diffusion of amorphous ^{11}B on ^{10}B in isotopically enriched thin films of ^{11}B/^{10}B on Si was investigated. It is rather surprising that since then practically no studies on self-diffusion measurements in me-

tallic multilayers using the neutron reflectivity technique were performed in spite of its unique potential. Another technique through which scattering contrast between two different isotopes of an element can be obtained is nuclear resonance reflectivity (NRR) of synchrotron radiation.[19,20] Possibility of using this technique for self-diffusion measurements of a Mössbauer active isotope was pointed out.[20] In a recent study this technique has been used to study self-diffusion of ^{57}Fe in some amorphous and nanocrystalline alloys.[21]

In the present study we have measured self-diffusion of iron in an isotopic multilayer of FeZr/^{57}FeZr in the amorphous state. The self-diffusion measurements have been carried out measuring the neutron reflectivity of the multilayer after isothermal vacuum annealing below the crystallization temperature. The height of the Bragg peak arising due to isotopic periodicity decays with annealing temperature and time and depicts the self-diffusion and the activation energy for a chemically homogeneous structure. In addition, a detailed fitting of the neutron reflectivity profile measured at room temperature yields interdiffusion at ambient conditions. The results of the obtained diffusion behavior are presented and discussed in this article.

II. EXPERIMENT

Amorphous FeZr isotopic multilayers have been prepared using a magnetron sputtering system. Natural Fe and ^{57}Fe enriched targets were sputtered alternatively to deposit the multilayer structure. The ^{57}Fe target was prepared by pasting a ^{57}Fe foil (^{57}Fe enrichment ~95%) onto a natural iron target. Small circular pieces of Zr (12 pieces) were pasted on the natural Fe as well as ^{57}Fe in an area ratio of Fe to Zr about 1:0.3. The multilayer with a nominal layer structure glass (substrate)/$[^{\text{natural}}\text{FeZr}(9\text{ nm})/^{57}\text{FeZr}(5\text{ nm})]_{20}$ was prepared. The composition of the film has been measured using x-ray photoelectron spectroscopy (XPS). The structural characterizations of the film have been carried out using x-ray reflectometry (XRR) and XRD techniques using a standard x-ray diffractometer and Cu $K\alpha$ radiation. Since the overall thickness of the film is relatively small, the XRD pattern of the film has been measured in the asymmetric Bragg–Brentano geometry at grazing incidence so that the background from the glass substrate can be minimized (keeping the incident angle just above the critical edge). Prior to diffusion measurements the crystallization behavior of the amorphous film has been studied using XRD after annealing the film isochronally in a vacuum furnace with a base vacuum of the order of 10^{-6} mbar.

The self-diffusion measurements have been carried out using neutron reflectivity after annealing the samples isothermally at four different temperatures. The neutron reflectivity measurements have been carried out in the time-of-flight mode on the AMOR reflectometer and in the θ-2θ mode on the MORPHEUS reflectometer both at SINQ/PSI.[22] With an incoming wavelength band of 0.2–0.9 nm the reflectivity pattern was measured using two different angular settings in the time of flight mode and on MORPHEUS using a monochromatic neutron beam with a wavelength of 0.474 nm.

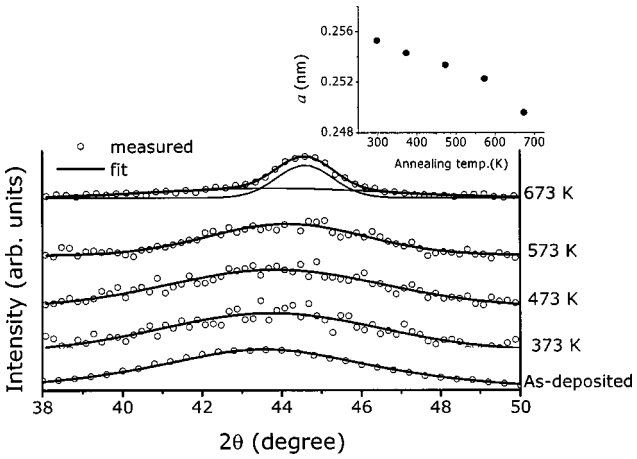

FIG. 1. X-ray diffraction pattern of the glass (substrate)/$[\text{FeZr}\ (9\text{ nm})/^{57}\text{FeZr}\ (5\text{ nm})]_{20}$ isotopic multilayer in the as-deposited state and after annealing at various temperatures as indicated in the figure. The measurements were carried out in the grazing incidence geometry using Cu $K\alpha$ x-rays. The inset in the figure shows the change in interatomic distance as a function of annealing temperature. The point corresponding to annealing at 673 K is after nanocrystallization.

III. RESULTS AND DISCUSSION

The composition of the cosputtered film was determined using XPS depth profiling. The average composition of the film was found to be $Fe_{67\pm3}Zr_{33\pm3}$ consistent with the area ratio of the targets used for sputtering. Figure 1 shows the x-ray diffraction pattern of the multilayer in the as-deposited state and after isochronal annealing in the temperature range of 373–673 K in a step of 100 K. The GIXRD pattern of the as-deposited film shows a broad hump centered around $2\theta = 44°$ which is typical for the iron based amorphous alloys.[1] The average interatomic distance can be estimated using the relation $a = 1.23\lambda/2\sin\theta$, where θ is taken to be the angle at the center of the amorphous hump, and the factor 1.23 is a geometric factor which rationalizes the nearest neighbor distance with the spacing between "pseudo-close packed planes."[23] The calculation gives an average interatomic distance in the present case equal to 0.255 ± 0.001 nm for the as-deposited sample. The inset in Fig. 1 shows the variation in the interatomic distance as a function of annealing temperature. As can be seen the interatomic distance shows a decrease with an increase of annealing temperature. Such a decrease indicates densification in the layer and is a direct consequence of structural relaxation which occurs due to annihilation of free volume during annealing. After annealing at 673 K, the amorphous hump converts into a relatively sharp peak indicating crystallization of the amorphous film. A detailed investigation of the peak shows that it is not possible to fit the peak using a single function, instead the best fit has been obtained using two Gaussian line shapes—one corresponding to the amorphous phase and the other to the crystalline bcc-Fe phase. This indicates that the film has not been crystallized completely and represents a mixture of amorphous and partially crystalline states. The width of the crystalline peak has been used to calculate the average grain

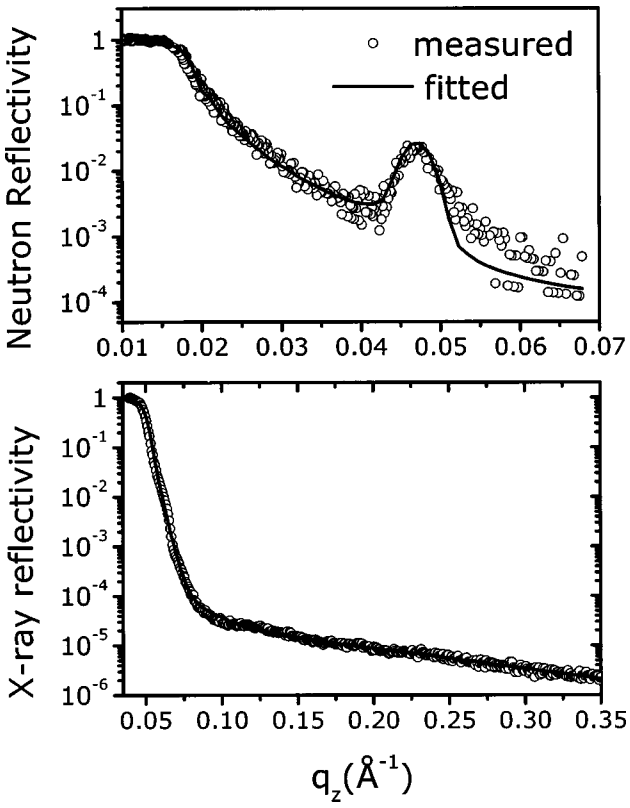

FIG. 2. Neutron (upper) and x-ray (below) reflectivity pattern of the $[\text{FeZr (9 nm)}/^{57}\text{FeZr(5 nm)}]_{20}$ isotopic multilayer. The neutron reflectivity pattern was measured in the time-of-flight mode on the AMOR reflectometer using an incoming wavelength band of 0.2–0.9 nm and using two angular settings. A Bragg peak corresponding to isotopic periodicity appears in the neutron reflectivity pattern while no such structure is visible for the x-rays. The x-ray reflectivity pattern was measured using Cu $K\alpha$ x-rays and standard θ-2θ geometry.

size using the Scherrer formula yielding a value of about 6 nm. The area ratio of the two components can be used to estimate the amount of crystallization which indicates that about 50% of the film has converted into the nanocrystalline phase.

Neutron reflectivity, in combination with x-ray reflectivity can be used to extract more information about the crystallization process of the amorphous multilayer. Figure 2 shows the neutron and the x-ray reflectivity pattern of the as-deposited multilayer. While a Bragg peak arising due to isotopic periodicity can be seen clearly in the neutron reflectivity pattern, no such structure can be seen in the x-ray reflectivity pattern. This shows that there is no chemical contrast between $^{\text{natural}}$FeZr and ^{57}FeZr, as expected. In fact, this is a prerequisite for studying self-diffusion in a chemically homogeneous multilayer as any chemical contrast would affect the diffusion process significantly and the measured diffusivity would no longer be self-diffusion but mediated by chemical inhomogeneity. The fitting of the neutron reflectivity data of the multilayer yields the following structure: Glass (substrate)/$[^{\text{natural}}\text{FeZr(9.1 nm)}/^{57}\text{FeZr(5.3 nm)}]_{20}$, which is close to the designed nominal structure. The neutron reflectivity pattern was fitted using a computer program

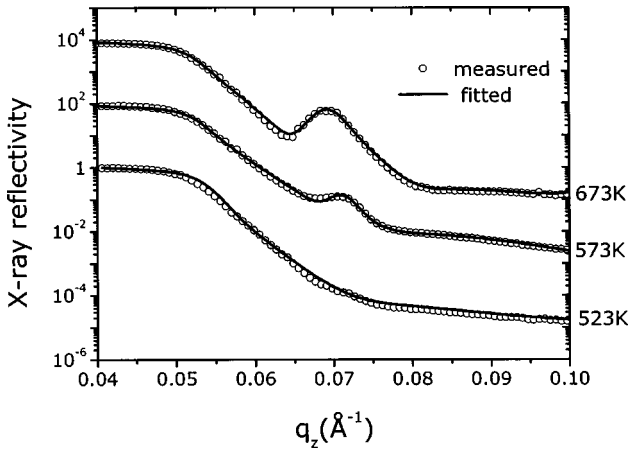

FIG. 3. X-ray reflectivity pattern of the isotopic multilayer after annealing at different temperatures. For 573 and 673 K patterns the intensity has been multiplied by a factor of 100 and 10 000, respectively, for clarity.

based on Parratt's formalism[24] and it was found that the pattern could not be fitted assuming sharp interfaces; instead a thin interlayer of thickness (0.8 ± 0.4) nm with the mean scattering length density of the two layers had to be introduced as interdiffused layer. This means that at room temperature there is some amount of interdiffusion in the multilayer. The x-ray reflectivity pattern was fitted assuming a single layer with a thin layer of scattering length density 50% of bulk layer, on the top of the film because of a possible oxidation of the film when exposed to the atmosphere.

Figure 3 shows the x-ray reflectivity pattern of the multilayer after annealing at 523, 573, and 673 K. It was observed that up to an annealing temperature of 523 K, the x-ray reflectivity pattern of the isotopic multilayer does not change significantly; only the thickness corresponding to the oxide layer is found to increase with annealing temperature. Whereas, after annealing at 573 K, a small Bragg peak appears indicating an evolution of chemical contrast between the natural and ^{57}Fe layers. Further annealing at 673 K sharpens this peak. As it is evident from the x-ray diffraction pattern of the multilayer that nanocrystalline Fe precipitates out from the amorphous phase after annealing at 673 K and the volume fraction of this nanocrystalline phase is about 50%. This information was taken as an input parameter while fitting the x-ray reflectivity pattern of the multilayer after annealing at 673 K. Two thin layers of pure iron (density 90–95% of bulk iron) were introduced on both sides of natural and ^{57}Fe layers with total thickness of this interlayer approximately equal to half of the bilayer thickness and this simple model, as shown in Fig. 4, gives a reasonably good fitting of the x-ray reflectivity pattern. Figure 5 shows the neutron reflectivity pattern of the multilayer after annealing at 573 and 673 K and for comparison in the as-deposited state (measured again in θ-2θ mode). Exactly the same model, as discussed above was applied for fitting the 673 K annealed neutron reflectivity pattern. Since neutrons have a significant contrast between $^{\text{natural}}$Fe and ^{57}Fe layers, the reflectivity at the Bragg peak should be more intense with neutrons as compared to x-rays. In the present case neutron

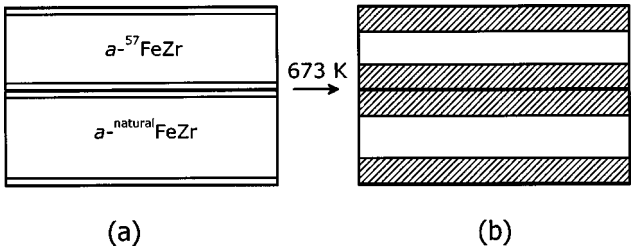

FIG. 4. Schematic diagram of the model used for fitting the x-ray and neutron reflectivity data: (a) represents the situation in the amorphous phase with a small interdiffusion but no chemical phase separation and (b) depicts the situation after nanocrystallization where Fe has precipitated out of the interfaces.

reflectivity was found to be more than 10 times in intensity with neutrons as compared with x-rays after annealing temperature of 673 K. In fact the neutron reflectivity for 673 K annealed sample is about 3 times higher in intensity as compared with that of the as-deposited sample. This indicates that upon nanocrystallization iron has precipitated out from the amorphous FeZr at the interfaces. The used model gives a reasonable fitting of both x-ray and neutron reflectivity data and is consistent with the XRD data. Therefore the crystallization process of the amorphous layers can be understood as a phase separation of iron from the amorphous phase at the interfaces. Due to the fact that the iron diffusivity is about 10^5 times higher[25] compared to that of zirconium, iron atoms would move much faster and precipitate out at the surface or interfaces upon crystallization. Using a model as discussed above, the x-ray reflectivity pattern of the multilayer annealed at 573 K can be fitted. It can be seen from the XRD data that the overall structure at 573 K is still amorphous; the volume fraction of the iron layer which would precipitate out at the interfaces should be very small. A thin layer of iron with a thickness (0.4 ± 0.2) nm gives a reasonably good fitting of the x-ray reflectivity pattern after annealing temperature of 573 K.

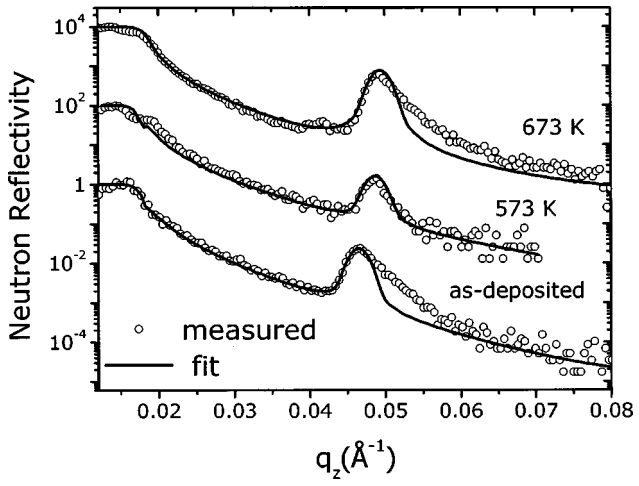

FIG. 5. Neutron reflectivity pattern of the isotopic multilayer after annealing at different temperatures. For the 573 and 673 K patterns the intensity has been multiplied by a factor of 10^2 and 10^4, respectively, for clarity.

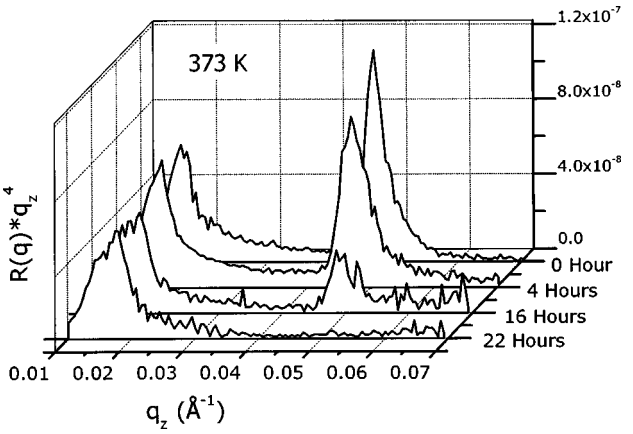

FIG. 6. Decay of Bragg peak intensity in the neutron reflectivity pattern of the $[\mathrm{FeZr(9\ nm)}/^{57}\mathrm{FeZr(5\ nm)}]_{20}$ isotopic multilayer after annealing at 373 K for different period of time.

Comparing the observed crystallization behavior with that reported in the literature, it can be seen that typical amorphous binary alloys that form a nanocrystalline microstructure have been found to crystallize in two steps. The primary crystallization reaction of amorphous alloys often leads to the evolution of nanocrystalline microstructures whereas the phase formed after the second stage results in an intermetallic compound along with nanocrystalline phase. The nominal reaction for such crystallization process had been given as: amorphous $\rightarrow \alpha+$amorphous $\rightarrow \alpha+\beta$; where α is the primary phase that precipitates out from the amorphous matrix and β is an intermetallic compound.[26,27] In the present case phase separation of iron from the amorphous layers could be described as the first stage of crystallization. However, no attempt has been made to study the second step of crystallization primarily because the aim of the present work is to study diffusion in the amorphous state only and second the samples in the present case were prepared on float glass substrates and for an annealing temperature higher than 700 K the glass substrate would melt.

Keeping in mind the above discussed crystallization behavior, the self-diffusion measurements have been performed at annealing temperatures of 523 K and below, so as to avoid crystallization of the amorphous layers during diffusion measurements. The diffusivity has been obtained after annealing the multilayer at 373, 423, 473, and 523 K for various periods of time. Figure 6 shows a typical decay of the Bragg peak intensity as a function of annealing time at 373 K. As can be seen, after an annealing time of 22 h the Bragg peak has completely vanished indicating that the whole layer has been diffused, while at initial times a shift of Bragg peak towards higher q values has been observed. This shift of the Bragg peak towards higher q would mean a reduction in the bilayer period and can be related to annihilation of free volume as a result of structural relaxation during annealing. A similar decay of the Bragg peak has been observed at abovementioned temperatures. The decay of the Bragg peak intensity can be used to calculate the diffusion coefficient using the expression:[28]

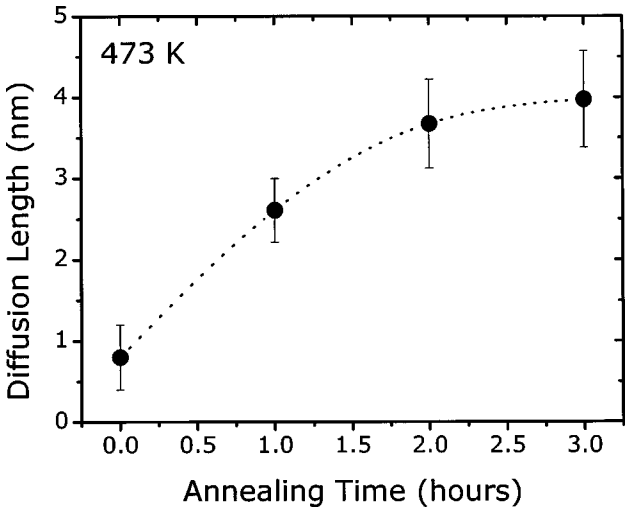

FIG. 7. Evolution of the diffusion length as a function of annealing time at 473 K. The diffusion length at room temperature has been obtained by fitting the neutron reflectivity data and at higher temperatures using Eq. (1). The dotted line is a guide to the eye.

$$\frac{d}{dt}\left[\ln\left(\frac{I(t)}{I_0}\right)\right] = -\frac{8\pi^2 n^2}{d^2} D(T), \tag{1}$$

where I_0 is the intensity of the nth order Bragg peak at time $t=0$; D is the diffusivity at the annealing temperature T, and d is the bilayer periodicity. The diffusion length L_d is related to the diffusivity $D(T)$, through the relation $L_d=\sqrt{4D(T)t}$; t being the annealing time.

The height of the Bragg peak was determined after subtracting the background due to Fresnel reflectivity by multiplying the data by a factor of q^4 (see Fig. 6), where q is the momentum transfer. Figure 7 shows the evolution of the diffusion length as a function of annealing time at 473 K. As can be seen, the diffusion length at longer annealing time does not increase linearly as compared to the diffusion length obtained at room temperature. A nonlinear increase in the diffusion length is not unexpected and essentially shows that the diffusion length increases much faster at a lower annealing time. Such an annealing time dependence of the diffusivity is attributed to structural relaxation in amorphous structures.[29,30] It may be noted that the maximum diffusion length that can be measured in the present case is limited by the thickness of the ^{57}FeZr layer. On achieving diffusion length of about 80% of the total layer thickness the diffusion length becomes almost constant. Therefore, at each temperature the annealing time was varied in order to achieve a diffusion length of 4 ± 0.2 nm. It is interesting to see that in order to achieve a constant diffusion length of 4 ± 0.2 nm, the required time decreases exponentially. A plot of the annealing temperature versus the annealing time is shown in Fig. 8, which has been used to obtain the average value of diffusivity over the annealing time. The values for the diffusivity obtained at four abovementioned temperatures were used to calculate the activation energy and the preexponential factor using the relation $D=D_0\exp(-E/k_BT)$, where D_0, E, and T are the preexponential factor, the activation energy and the annealing temperature respectively and k_B is the Boltzmann constant. Figure 9 shows a plot of the diffusion coefficient versus the inverse of temperature, which follows the Arrhenius type behavior. The calculated values of D_0 and the activation energy E are $5\times10^{-18\pm1}$ m^2 s^{-1} and 0.38 ± 0.05 eV, respectively. It may be noted that the values of both the preexponential factor and the activation energy are significantly smaller in the present case as compared with that of iron based amorphous alloys, e.g., for Fe diffusion in a-$Fe_{91}Zr_9$ $D_0=3.1\times10^{-7}$ m^2 s^{-1} and $E=1.45$ eV.[31,32] On the other hand, the values obtained in the present case follow the well-known correlation between D_0 and E for self and impurity diffusion in conventional and bulk amorphous alloys.[2,15,33,34] This relationship seems to have a universal character as it has been observed not only for self and impurity diffusion in amorphous alloys but also in nanocrystalline and crystalline alloys.[34]

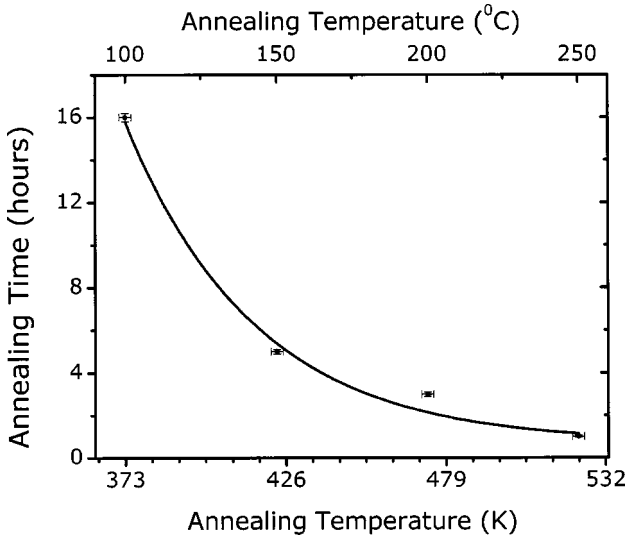

FIG. 8. Annealing time required to achieve a constant diffusion length of 4 ± 0.2 nm at different annealing temperatures. The solid line is a guide to the eye.

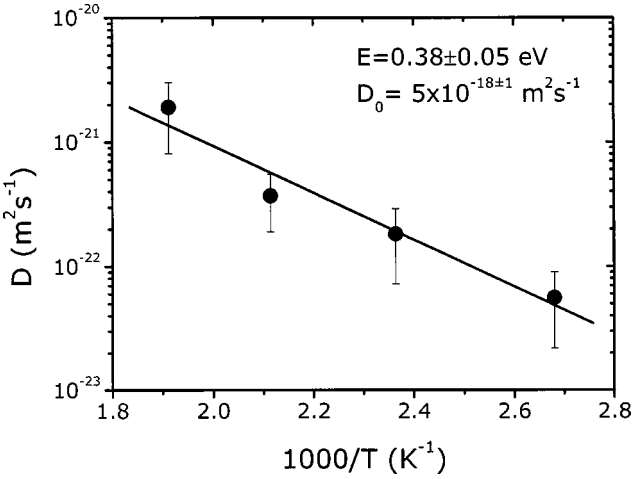

FIG. 9. Arrhenius behavior of the diffusivity. The solid circles represent the average diffusivity at a given temperature obtained using the data of Fig. 8. Solid line has been obtained using the equation: $D=D_0\exp(-E/k_BT)$.

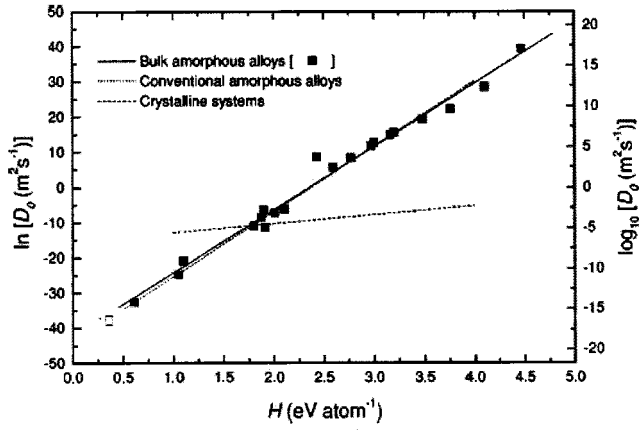

FIG. 10. Correlation between the preexponential factor D_0 and the activation energy E for amorphous and crystalline alloys (taken from Ref. 2); (□) corresponds to the present study.

The data point corresponding to the present study is shown in Fig. 10 along with the values obtained in the literature.[2] The relationship between D_0 and E is known as isokinetic relation and is given by:[35]

$$\ln D_0 = \ln A + \frac{E}{B}, \tag{2}$$

where A and B are constants. Taking our data point into account (as shown in Fig. 10) we find the values for A and B equal to 2×10^{-20} and 0.056, respectively, which are very close to the values obtained for diffusion in amorphous alloys[2] and interdiffusion in chemically inhomogeneous metallic multilayers.[15] Following the approach as discussed by Shewmon[36] the preexponential factor D_0 can be expressed as:

$$\ln D_0 = \ln(ga^2 f \upsilon_0) + \left(\frac{\Delta S}{k_B}\right), \tag{3}$$

where g is a geometry factor, a the effective jump distance, υ_0 the effective jump attempt frequency, f the correlation factor, and ΔS the entropy for diffusion. Using Eqs. (2) and (3) the values for the constants A and B can be written as:

$$A = ga^2 f \upsilon_0, \quad B = k_B E/\Delta S. \tag{4}$$

With the calculated values of B and E the entropy term ΔS for the present sample would be about $7k_B$, which is much smaller as compared to $19k_B-56k_B$ observed for amorphous alloys and close to the value of $8k_B-15k_B$ obtained for interdiffusion in chemically inhomogeneous multilayers. The value of $7k_B$ would roughly correspond to a cluster of seven atoms[15] that may move through the defects. This would mean that diffusion in the chemically homogeneous multilayer would not be highly collective but would involve a relatively small group of atoms, indicating a much faster diffusion as compared with that of bulk amorphous alloys. The values obtained in the present case can be compared with the values obtained for iron self-diffusion in amorphous $^{57}Fe_{70}Zr_{30}$ (3 nm)/$Fe_{70}Zr_{30}$ (4 nm) isotopic multilayer, prepared by ion beam sputtering and measured by nuclear resonance reflectivity of synchrotron radiation.[21] The obtained values of the activation energy and the preexponential factor were, $E=0.42$ eV and $D_0=1\times10^{-17}$ m^2 s^{-1} which are within experimental errors comparable to the values obtained in the present case.

There has been much discussion in the literature regarding the effect of preparation techniques on the diffusivity. For example, in a number of studies[37,38] diffusivity of a number of impurities like Au, Cu, Fe, and Ti has been measured for amorphous films of NiZr produced by coevaporation. In these films no variation of the diffusivity was observed with structural relaxation. The authors attributed this to the fact that the evaporation produced well relaxed samples. Furthermore, Faupel *et al.*,[39,40] found a significant isotope effect in the diffusivity of Co in melt-spun amorphous $Co_{76.7}Fe_2Nb_{14.3}B_7$ while in sputter deposited amorphous $Co_{51}Zr_{49}$ no isotope effect was observed. This difference was again attributed to a difference in the structure of as prepared melt-spun and sputter deposited amorphous alloy. In this context it is interesting to observe that in the present case, the films produced by two different techniques, namely magnetron sputtering and ion beam sputtering have similar diffusivity, suggesting that they are similar in structure.

IV. CONCLUSIONS

In the present work self-diffusion of iron in chemically homogeneous amorphous $Fe_{67}Zr_{33}$ isotopic multilayers has been measured by neutron reflectivity. Careful examination of the isotopic multilayer structure with neutron and x-ray reflectivity reveals that even after the longest annealing times no chemical inhomogeneity develops in the multilayer below an annealing temperature of 523 K. Above this temperature the phase separation of Fe starts at 573 K and at 673 K about half of the amorphous structure precipitates out in nanocrystalline grains of iron at the interfaces. The activation energy (E), and the prefactor for diffusion (D_0) in the system supports the universal type $E-D_0$ correlation. This correlation along with the observed value of the activation energy suggests that the diffusion mechanism in the present case is not highly collective in contrast to melt spun metallic glasses; instead it involves only a small group of atoms.

ACKNOWLEDGMENTS

Thanks are due to Dr. Fabio Raimondi, General Energy Research, Paul Scherrer Institute, for providing help in x-ray photoelectron spectroscopy measurements.

*Corresponding author. E-mail: mukul.gupta@psi.ch

[1] M. E. McHenry, M. A. Willard, and D. E. Laughlin, Prog. Mater. Sci. **44**, 291 (1999).
[2] F. Faupel, W. Frank, M.-P. Macht, H. Mehrer, V. Naundorf, K. Rätzke, H. R. Schober, S. K. Sharma, and H. Teichler, Rev. Mod. Phys. **75**, 237 (2003).
[3] A. L. Greer and F. Spaepen, in *Synthetic Modulated Structures*, edited by L. L. Chang and B. C. Giessen (Academic, New York, 1985), pp. 419–486.
[4] U. Geyer, S. Schneider, W. L. Johnson, Y. Qiu, T. A. Tombrello, and M.-P. Macht, Phys. Rev. Lett. **75**, 2364 (1995); P. Fielitz, M.-P. Macht, V. Naundorf, and G. Frohberg, J. Non-Cryst. Solids **250-252**, 674 (1999).
[5] F. Faupel, P. W. Hüppe, and K. Rätzke, Phys. Rev. Lett. **65**, 1219 (1990).
[6] K. Knorr, M.-P. Macht, K. Freitag, and H. Mehrer, J. Non-Cryst. Solids **250**, 669 (1999).
[7] K. N. Tu and T. C. Chou, Phys. Rev. Lett. **61**, 1863 (1988); H. Hahn and R. S. Averback, Phys. Rev. B **37**, 6533 (1988); J. C. Barbour, F. W. Saris, M. Nastasi, and J. W. Mayer *et al.*, Phys. Rev. B **32**, 1363 (1985).
[8] P. Klugkist, K. Rätzke, and F. Faupel, Phys. Rev. Lett. **81**, 614 (1998); W. Dörner and H. Mehrer, Phys. Rev. B **44**, 101 (1991).
[9] O. Le Bacq, F. Willaime, and A. Pasturel, Phys. Rev. B **59**, 8508 (1999).
[10] J. Drinklage and R. Frerichs, J. Appl. Phys. **34**, 2633 (1963).
[11] H. E. Cook and J. E. Hilliard, J. Appl. Phys. **40**, 2191 (1969).
[12] M. P. Rosenblum and D. Turnbull, Appl. Phys. Lett. **37**, 184 (1980).
[13] A. L. Greer, Defect Diffus. Forum **143-147**, 557 (1997).
[14] T. Mizoguchi, S. Tanbe, and M. Murata, J. Magn. Magn. Mater. **126**, 96 (1993).
[15] W.-H. Wang, H. Y. Bai, M. Zhang, J. H. Zhao, X. Y. Zhang, and W. K. Wang, Phys. Rev. B **59**, 10 811 (1999).
[16] A. L. Greer, J. Magn. Magn. Mater. **126**, 89 (1993); J. Speakman, P. Rose, J. A. Hunt, N. Cowlam, R. E. Somekh, and A. L. Greer *et al.*, J. Magn. Magn. Mater. **156**, 411 (1996).
[17] A. L. Greer, Defect Diffus. Forum **129-130**, 163 (1996).
[18] S. M. Baker, G. S. Smith, N. J. S. Brown, M. Nastasi, and K. Hubbard, Phys. Rev. B **55**, 7255 (1997).
[19] A. I. Chumakov and G. V. Smirnov, JETP Lett. **53**, 273 (1991).
[20] A. Gupta, M. Gupta, B. A. Dasannacharya, S. Kikuta, Y. Yoda, and M. Seto, J. Phys. Soc. Jpn. **73**, 423 (2004).
[21] A. Gupta, M. Gupta, S. Chakravarty, R. Rüffer, H.-C. Wille, and O. Leupold (unpublished).
[22] M. Gupta, T. Gutberlet, J. Stahn, P. Keller, and D. Clemens, Pramana, J. Phys. **63**, 57 (2004); D. Clemens *et al.*, Physica B **276-278**, 140 (2000).
[23] A. Guinier, *X-Ray Diffraction: In Crystals, Imperfect Crystals and Amorphous Bodies* (Dover, New York, 1994).
[24] L. G. Parratt, Phys. Rev. **95**, 359 (1954).
[25] A. L. Greer, N. Karpe, and J. Bøttiger, J. Alloys Compd. **194**, 199 (1993).
[26] K. Hono and D. H. Ping, Mater. Charact. **44**, 203 (2000).
[27] D. M. Zhu, K. Raviprasad, K. Suzuki, and S. P. Ringer, J. Phys. D **37**, 645 (2004).
[28] J. Speakman, P. Rose, J. A. Hunt, N. Cowlam, R. E. Somekh, and A. L. Greer, J. Magn. Magn. Mater. **156**, 411 (1996).
[29] Y. Loirat, J. L. Boequet, and Y. Limoge, J. Non-Cryst. Solids **265**, 252 (2000).
[30] M. Gupta, A. Gupta, S. Rajagopalan, and A. K. Tyagi, Phys. Rev. B **65**, 214204 (2002).
[31] J. Horvath, J. Ott, K. Pfahler, and W. Ulfert, Mater. Sci. Eng. **97**, 409 (1988).
[32] H. Kronmüller and W. Frank, Radiat. Eff. Defects Solids **108**, 81 (1989).
[33] S. K. Sharma, M.-P. Macht, and V. Naundorf, Phys. Rev. B **49**, 6655 (1994).
[34] V. Naundorf, M.-P. Macht, A. S. Bakai, and N. Lazarev, J. Non-Cryst. Solids **250-252**, 679 (1999).
[35] W. Linert, Chem. Soc. Rev. **18**, 477 (1989).
[36] P. G. Shewmon, *Diffusion in Solids* (Minerals, Metals, and Materials Society, Warrendale, PA, 1989).
[37] K. Hoshino, R. S. Averback, H. Hahn, and S. J. Rothman, Defect Diffus. Forum **A59**, 225 (1988).
[38] H. Hahn, R. S. Averback, and H. M. Shyu, J. Less-Common Met. **140**, 345 (1988).
[39] F. Faupel, K. Ratzke, and P. W. Huppe, Defect Diffus. Forum **95-98**, 1175 (1993).
[40] V. Zollmer, H. Ehmler, K. Rätzke, P. Troche, and F. Faupel, Europhys. Lett. **51**, 75 (2000).